

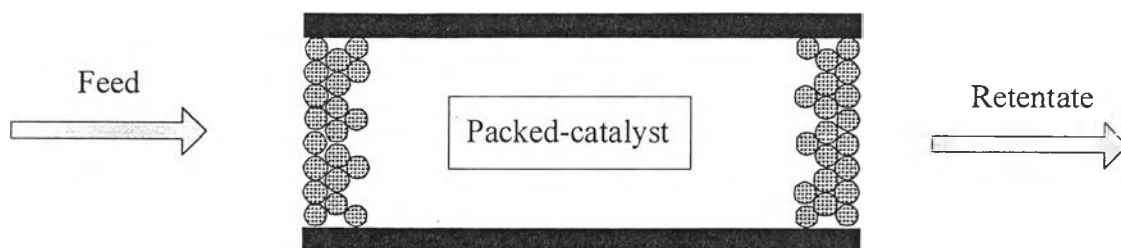
CHAPTER IV

MATHEMATICAL MODEL

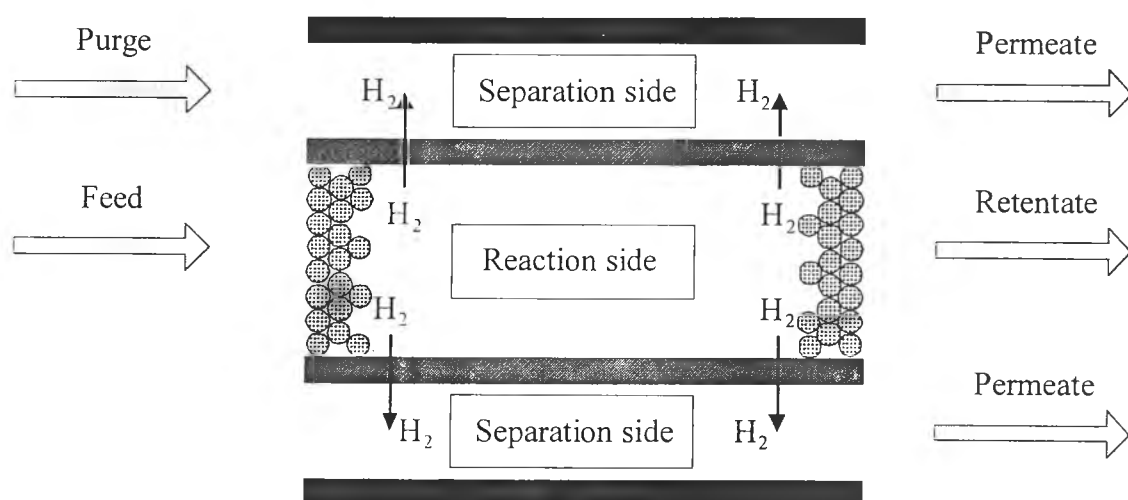
The research studied the dehydrogenation of ethylbenzene to styrene in fixed-bed reactors and palladium membrane reactors. Industrially, the reaction is carried out in the presence of large amounts of steam. In conventional fixed-bed reactor, the feed was mixture of steam and ethylbenzene. A system of six reactions was used to represent the industrial process of dehydrogenation of ethylbenzene. The rate expressions of the commercial catalyst consisting of Fe_2O_3 and K_2O were obtained by Abdalla *et al.* (1993, 1994a and 1994b). More information about the kinetic data is given in Appendix A. The membrane reactor consists of two concentric tubes: the inner one is the membrane, whereas the outer is a stainless steel shell. The elements of the membrane used in this research consisted of a very thin dense film of palladium deposited on a tubular support of alumina, the detail on the membrane is described in Appendix B. The reaction side may be either in the tube side or in the shell side (see Figure 4.1). In the separation side three different process options; i.e., the use of an inert sweep gas, vacuum mode and the use of a reactive sweep gas, can be employed.

The palladium composite membrane was pin-hole free and permeable to hydrogen only. The permeation rate of hydrogen gas through the palladium composite membrane, Q_H , was assumed to obey the half-power pressure by Sieverts' s law. Hydrogen permeation through the membrane is based on the permeation data of hydrogen through a commercial palladium membrane (Hermann *et al.* 1997). The expression for hydrogen permeation rate is given by

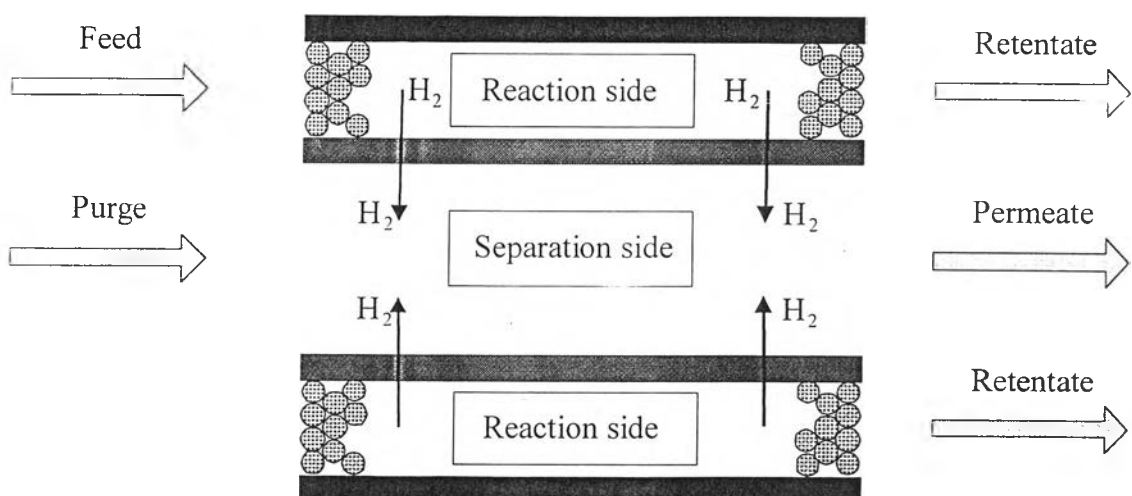
$$Q_H = \alpha_H \left[P_{H_2,R}^{0.5} - P_{H_2,S}^{0.5} \right] \quad (4.1)$$



a) Fixed-bed reactor



b) catalyst packed in tube side of membrane reactor



c) catalyst packed in shell side of membrane reactor

Figure 4.1 Schematic diagrams of fixed-bed reactor and membrane reactor.

Details of the hydrogen permeation rate are given in Appendix B.

Pseudo-homogeneous models for both cases of with and with out radial effect were developed by using the following assumptions:

1. operation is at steady state condition;
2. the ideal gas behavior is assumed to determine the properties of gas;
3. pressure is constant in the catalyst bed. neglecting pressure drop;
4. temperature at the wall of reactor is constant;
5. axial dispersion of mass and heat are neglected;
6. interfacial mass transfer resistance between the gas and the surface of membrane is small compared with the internal mass transfer resistance in the membrane;
7. membrane is catalytically inactive;
8. any change in pressure in the sweep gas due to hydrogen permeation may be neglected because of the small extent of permeation compared to the sweep flow rate.

In this chapter, the development of mathematical models is classified into two parts; plug-flow model and radial diffusion model. Details of the development of conventional fixed-bed reactor and membrane reactor models are given in Appendix C and D, respectively. For the plug flow model the 4th order Runge-Kutta method was employed to integrate a set of ordinary differential equations while the method of line was used for the radial model to integrate a set of partial differential equations. The EQUATRAN-G program was employed for performing simulation. The followings summarize the sets of equations for both reactors and both models.

4.1 Plug-flow model

In most simulations of conventional packed-bed reactor and membrane reactor the assumption of plug-flow condition for fluid is generally considered.

4.1.1 Conventional fixed-bed reactor

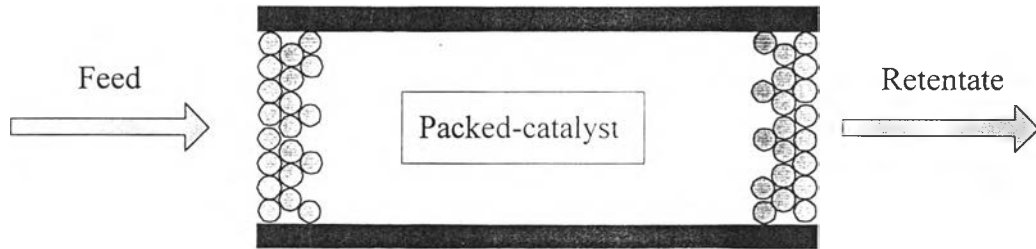


Figure 4.2 Conventional fixed-bed reactor.

A set of differential equations for each component in conventional fixed-bed reactor (Figure 4.2) in dimensionless forms can be derived through the material and energy balances.

Material balance :

$$\frac{d\bar{M}_i}{dL} = c_1 r_i \quad (4.2)$$

Energy balance :

$$\sum (M_i c_{p,i}) \frac{d\bar{T}}{dL} = \underbrace{c_2 (\bar{T}_{ss} - \bar{T})}_{\text{Heat transfer through stainless steel}} + \underbrace{c_3 \sum (r_i \times \Delta H_{R,i})}_{\text{Heat of reaction}} \quad (4-3)$$

where $c_1 = \frac{\rho_c A_c l_0}{M_{T,0}}$

$$c_2 = U_{ss} 2\pi r_1 l_0$$

$$c_3 = \pi r_1^2 l_0 \rho_c$$

4.1.2 Membrane reactor

The catalyst is assumed to be loaded in the shell side of the membrane reactor.

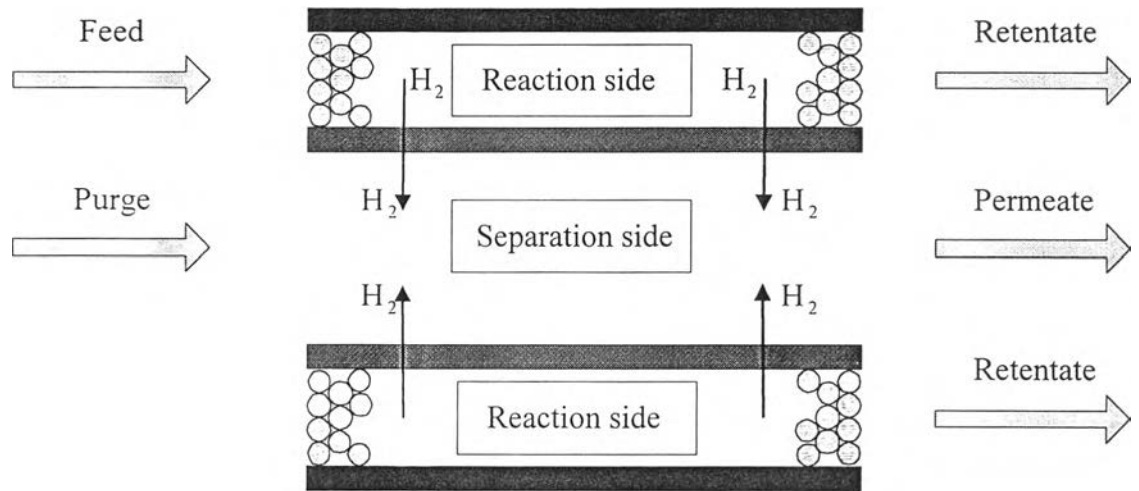


Figure 4.3 Membrane reactor.

Figure 4.3 shows the flow model of components in the membrane reactor. Plug-flow condition was assumed in both sides of the membrane. A set of differential equations for each component in dimensionless form can be derived as.

Material balance :

Reaction side :

$$\frac{d\bar{M}_i^s}{dL} = a_1 r_i - a_2 Q_H \quad (4-4)$$

Permeation side :

$$\frac{d\bar{M}_i^r}{dL} = a_7 Q_H \quad (4-5)$$

Energy balance :

Reaction side:

$$\sum (M_i^S C_{P,i}^S) \frac{d\bar{T}^S}{dL} = a_3(\bar{T}_{SS} - \bar{T}^S) + a_4(\bar{T}^T - \bar{T}^S) + a_5 \sum (r_i \times \Delta H_{R,i}) + a_6 H_m^S Q_H \quad (4-6)$$

Heat transfer
Heat transfer
Heat of reaction
Heat
through stainless steel
through membrane
transfer by permeation gas

permeation side:

$$\sum (\bar{M}_i^T C_{p,i}^T) \frac{d\bar{T}^T}{dL} = -a_8(\bar{T}^T - \bar{T}^S) - a_9 H_m^T Q_H \quad (4.7)$$

heat transfer
heat transfer
through membrane
by mass permeation

where

$$a_1 = \frac{\rho_c A_c^S l_0}{M_{T,0}^S} ; a_2 = \frac{l_0}{M_{T,0}^S} ; a_3 = U_{SS} 2\pi r_3 l_0 ; a_4 = U_m 2\pi r_1 l_0 ;$$

$$a_5 = \frac{A_c l_0 \rho_c}{T_0^S} ; a_6 = \frac{l_0}{T_0^S} ; a_7 = \frac{l_0}{M_{T,0}^T} ; a_8 = U_m 2\pi r_1 l_0 ; a_9 = \frac{l_0}{T_0^T}$$

4.2 Radial diffusion model

4.2.1 Conventional fixed-bed reactor

From the material balance, the basic partial differential equations of the radial models for conventional packed-bed reactors are as follows:

Material balance:

$$\frac{\partial \bar{M}_i}{\partial L} = c_4 \left[\frac{1}{R} \frac{\partial}{\partial R} \left(\frac{\bar{M}_i}{M_T T} \right) + \frac{\partial^2}{\partial R^2} \left(\frac{\bar{M}_i}{M_T T} \right) \right] + c_5 r_i$$

Boundary conditions:

$$\begin{aligned} \text{at : } L = 0 ; & \quad \bar{M}_i = \bar{M}_{i,0} \quad (0 < R < 1) \\ R = 0 ; & \quad \left. \frac{\partial}{\partial r} \left(\frac{\bar{M}_i}{M_T T} \right) \right|_{r=0} = 0 \quad (0 < L < 1) \\ R = 1 ; & \quad \left. \frac{\partial}{\partial r} \left(\frac{\bar{M}_i}{M_T T} \right) \right|_{r=1} = 0 \quad (0 < L < 1) \end{aligned} \quad (4-8)$$

Energy balance:

$$\frac{\partial \bar{T}}{\partial L} = c_6 \left[\frac{1}{R} \frac{\partial \bar{T}}{\partial R} + \frac{\partial^2 \bar{T}}{\partial R^2} \right] + c_7 \Sigma (r_i \times \Delta H_{R,i})$$

Boundary conditions:

$$\begin{aligned} \text{At : } L = 0 ; & \quad \bar{T} = 1 \quad (0 < R < 1) \\ R = 0 ; & \quad \frac{\partial \bar{T}}{\partial R} = 0 \\ R = 1 ; & \quad 2\pi L \lambda_{er} \frac{\partial \bar{T}}{\partial R} = 2\pi r_1 L U_{SS} (\bar{T}_{SS} - \bar{T}_{R=1}) \end{aligned} \quad (4-9)$$

where

$$c_4 = \frac{D_{cr} A_c I_0 P_T}{F_{T,0} T_0 R r_1^2}$$

$$c_5 = \rho_c \left(\frac{A_c I_0}{F_{T,0}} \right);$$

$$c_6 = \frac{\lambda_{er} l_0}{r_1^2} \frac{A_c}{\sum(C_{p,i} M_i)} \quad \text{and}$$

$$c_7 = \rho_c \frac{l_0}{T_0} \frac{A_c}{\sum(C_{p,i} M_i)}$$

4.2.2 Membrane reactor

A set of partial differential equations of the radial diffusion models for both sides of the membrane are as follows:

Material balance:

Reaction side:

$$\frac{\partial \bar{M}_i^S}{\partial L} = a_{S,1} \left[\frac{1}{R^S + R_2} \frac{\partial}{\partial R^S} \left(\frac{\bar{M}_i^S}{\bar{M}_T^S \bar{T}^S} \right) + \frac{\partial^2}{\partial R^{S2}} \left(\frac{\bar{M}_i^S}{\bar{M}_T^S \bar{T}^S} \right) \right] + a_{S,2} r_i$$

Boundary conditions:

$$\text{at : } L = 0 ; \quad \bar{M}_i^S = \bar{M}_{i,0}^S \quad (0 < R^S < 1)$$

$$R^S = 0 ; \quad D_{er}^S \frac{P_S}{RT_0^S} \frac{\partial}{\partial R^S} \left(\frac{\bar{M}_i^S}{\bar{M}_T^S \bar{T}^S} \right) = \frac{l_0}{2\pi r_2 l_0} Q_H \quad (0 < l_0 < 1) \quad (4-10)$$

$$R^S = 1 ; \quad \frac{\partial}{\partial R^S} \left(\frac{\bar{M}_i^S}{\bar{M}_T^S \bar{T}^S} \right) = 0 \quad (0 < l_0 < 1)$$

Separation side:

$$\frac{\partial \bar{M}_i^T}{\partial L} = a_{T,1} \left[\frac{1}{R^T} \frac{\partial}{\partial R^T} \left(\frac{\bar{M}_i^T}{\bar{M}_T^T \bar{T}^T} \right) + \frac{\partial^2}{\partial R^{T2}} \left(\frac{\bar{M}_i^T}{\bar{M}_T^T \bar{T}^T} \right) \right]$$

Boundary conditions:

$$\text{at : } L = 0 ; \quad \bar{M}_i^T = \bar{M}_{i,0}^T \quad (0 < R^T < 1)$$

$$R^T = 1 ; \quad D_{er}^T \frac{P_T}{RT_0^T} \frac{\partial}{\partial R^T} \left(\frac{\bar{M}_i^T}{\bar{M}_T^T \bar{T}^T} \right) = \frac{l_0}{2\pi r_1 l_0} Q_H \quad (0 < l_0 < 1) \quad (4-11)$$

$$R^T = 0 ; \quad \frac{\partial}{\partial R^T} \left(\frac{\bar{M}_T}{M_T \bar{T}^T} \right) = 0 \quad (0 < l_0 < 1)$$

Energy balance:

Reaction side:

$$\frac{\partial \bar{T}^S}{\partial L} = a_{S,3} \left[\frac{1}{R^S + R_2} \frac{\partial \bar{T}^S}{\partial R^S} + \frac{\partial^2 \bar{T}^S}{\partial R^{S2}} \right] + a_{S,4} \Sigma (r_i \times \Delta H_{R,i})$$

Boundary conditions:

$$\text{At: } L = 0 ; \quad \bar{T}^S = 1 \quad (0 < R^S < 1)$$

$$R^S = 0 ; \quad \frac{\partial \bar{T}^S}{\partial R^S} = a_{S,5} U_m (\bar{T}^T - \bar{T}^S) + a_{S,5} \frac{l_0}{2\pi r_2 l_0 T_0^S} Q_H \quad (0 < l_0 < 1) \quad (4-12)$$

$$R^S = 1 ; \quad \frac{\partial \bar{T}^S}{\partial R^S} = a_{S,5} U_{ss} (\bar{T}_{ss} - \bar{T}_{R=1}^S) \quad (0 < l_0 < 1)$$

Separation side :

$$\frac{\partial \bar{T}^T}{\partial L} = a_{T,2} \left[\frac{1}{R^T} \frac{\partial \bar{T}^T}{\partial R^T} + \frac{\partial^2 \bar{T}^T}{\partial R^{T2}} \right]$$

Boundary conditions:

$$\text{At: } L = 0 ; \quad \bar{T}^T = 1 \quad (0 < R^T < 1)$$

$$R^T = 1 ; \quad \frac{\partial \bar{T}^T}{\partial R^T} = -a_{T,3} U_m (\bar{T}^T - \bar{T}^S) - a_{T,3} \frac{l_0}{2\pi r_1 l_0 T_0^T} Q_H \quad (0 < l_0 < 1) \quad (4-13)$$

$$R^T = 0 ; \quad \frac{\partial \bar{T}^T}{\partial R^T} = 0 \quad (0 < l_0 < 1)$$

Where

$$a_{S,1} = \frac{D_{er}^S \times \pi l_0 P_S}{T_0^S F_{T,0}^S R} ; \quad a_{S,2} = \rho_c \left(\frac{A_C^S l_0}{F_{T,0}^S} \right) ; \quad a_{S,3} = \frac{l_0 \pi \lambda_{er}^S}{\Sigma (F_{T,0}^S C_{P,i}^S)} ;$$

$$\begin{aligned}
 a_{S,4} &= \rho_c \frac{A_C^S l_0}{T_0^S} \frac{1}{\Sigma(F_{T,0}^S C_{p,i})}; & a_{S,5} &= \frac{A_C^S}{\lambda_{er}^S \pi}; \\
 a_{T,1} &= \frac{D_{er}^T \times \pi l_0 P_T}{T_0^T F_{T,0}^T R}; & a_{T,2} &= \frac{l_0 \pi \lambda_{er}^T}{\Sigma(F_{T,0}^T C_{p,i})}; & a_{S,3} &= \frac{A_C^T}{\lambda_{er}^T \pi}
 \end{aligned}$$